CORE
Metadata, citation and similar papers at core.ac.uk
Provided by Elsevier - Publisher Connector

ARTICLE

A BLOC-1 Mutation Screen Reveals that *PLDN* Is Mutated in Hermansky-Pudlak Syndrome Type 9

Andrew R. Cullinane,[1,*] James A. Curry,[1] Carmelo Carmona-Rivera,[1] C. Gail Summers,[2] Carla Ciccone,[1] Nicholas D. Cardillo,[1] Heidi Dorward,[1] Richard A. Hess,[1] James G. White,[3] David Adams,[1,4] Marjan Huizing,[1] and William A. Gahl[1,4]

Hermansky-Pudlak Syndrome (HPS) is an autosomal-recessive condition characterized by oculocutaneous albinism and a bleeding diathesis due to absent platelet delta granules. HPS is a genetically heterogeneous disorder of intracellular vesicle biogenesis. We first screened all our patients with HPS-like symptoms for mutations in the genes responsible for HPS-1 through HPS-6 and found no functional mutations in 38 individuals. We then examined all eight genes encoding the *b*iogenesis of *l*ysosome-related *o*rganelles *c*omplex-1, or BLOC-1, proteins in these individuals. This identified a homozygous nonsense mutation in *PLDN* in a boy with characteristic features of HPS. *PLDN* is mutated in the HPS mouse model *pallid* and encodes the protein pallidin, which interacts with the early endosomal t-SNARE syntaxin-13. We could not detect any full-length pallidin in our patient's cells despite normal mRNA expression of the mutant transcript. We could detect an alternative transcript that would skip the exon that harbored the mutation, but we demonstrate that if this transcript is translated into protein, although it correctly localizes to early endosomes, it does not interact with syntaxin-13. In our patient's melanocytes, the melanogenic protein TYRP1 showed aberrant localization, an increase in plasma-membrane trafficking, and a failure to reach melanosomes, explaining the boy's severe albinism and establishing his diagnosis as HPS-9.

Introduction

Hermansky-Pudlak Syndrome (HPS; MIM 203300) is a rare autosomal-recessive condition characterized by reduced skin, hair, and eye pigmentation and a bleeding diathesis due to absent platelet delta granules. Occasionally, HPS patients are found to have additional symptoms, including pulmonary fibrosis, granulomatous colitis, and immunodeficiency.[1] To date, eight HPS subtypes (HPS1–8; MIM 604982, 608233, 606118, 606682, 607521, 607522, 607145, and 609762) and genes have been identified in humans;[2–8] their protein products are involved in the biogenesis of lysosome-related organelles such as melanosomes in melanocytes and delta granules in platelets.[1,9,10] All known HPS proteins are components of one of four protein complexes: BLOC-1, BLOC-2, BLOC-3, or *A*daptor *P*rotein Complex-3 (AP-3).

BLOC-1 contains eight subunits: BLOC1S1, BLOC1S2, BLOC1S3 (HPS8), cappuccino, dysbindin (HPS7), muted, pallidin, and snapin (MIM 601444, 609768, 609762, 605695, 607145, 607289, 604310, and 607007, respectively). HPS mouse models exist for mutations in five of the eight BLOC-1 subunits.[11] Relatively little is known about the exact subcellular function of the BLOC-1 complex constituents. However, interaction of the snapin subunit with the t-SNARE SNAP25 suggests a role in synapse function in neuronal tissues. In nonneuronal tissue, snapin interacts with the SNAP25 counterpart, SNAP23,[12] and the pallidin subunit interacts with the early endosomal t-SNARE Syntaxin-13;[13] both interactions suggest a role in endosomal protein sorting.

Only two human families with BLOC-1 defects are known.[7,8] Specifically, HPS-7 and HPS-8 involve mutations in *dysbindin* and *BLOC1S3*, respectively. In the current study, we screened patients with clinical findings suggestive of HPS for mutations in additional BLOC-1 subunits and identified a single individual with a mutation in the *PLDN* gene encoding the pallidin subunit of BLOC-1, and these findings define the HPS-9 subtype.

Material and Methods

Patients

All 38 patients were enrolled in either clinical protocol NCT00001456 "Clinical and Basic Investigations into Hermansky-Pudlak Syndrome," or protocol NCT00369421, "Diagnosis and Treatment of Inborn Errors of Metabolism and Other Genetic Disorders," approved by the NHGRI Institutional Review Board. All patients or their parents provided written, informed consent. The HPS-9 patient was enrolled in protocol NCT00369421, and written, informed consent was obtained from his parents.

Tissue Culture

Primary patient and control fibroblasts and melanocytes were cultured from a forearm skin biopsy. Fibroblasts were grown in high-glucose (4.5 g/liter) DMEM medium supplemented with 10% fetal calf serum (FCS; Gemini Bio-Products, West Sacramento, CA), 2 mM L-glutamine, MEM nonessential amino acid solution, and penicillin-streptomycin. Melanocytes were cultured in Ham's F10 (Invitrogen, Carlsbad, CA), supplemented with 5% FCS, 5 μg/liter basic fibroblast growth factor (Sigma, St. Louis, MO), 10 μg/liter endothelin (Sigma), 7.5 mg/liter 3-isobutyl-1-methylxanthine (Sigma), 30 μg/liter choleratoxin (Sigma),

[1]Medical Genetics Branch, National Human Genome Research Institute, National Institutes of Health, Bethesda, MD 20892, USA; [2]Departments of Ophthalmology and Pediatrics, University of Minnesota, Minneapolis, MN 55455, USA; [3]Department of Laboratory Medicine, University of Minnesota, Minneapolis, MN 55455, USA; [4]Intramural Office of Rare Diseases Research, Office of the Director, National Institutes of Health, Bethesda, MD 20892, USA
*Correspondence: andrew.cullinane@nih.gov
DOI 10.1016/j.ajhg.2011.05.009. ©2011 by The American Society of Human Genetics. All rights reserved.

3.3 μg/liter phorbol 12-myristate 13-acetate (Sigma), 10 ml pen/strep/glutamine (Invitrogen) and 1 ml fungizone (Invitrogen). Melanocytes were transfected with 1 μg of cDNA constructs via the Amaxa nucleofection system (Lonza, Walkersville, MD).

gDNA Analysis: Sequencing and SNP Array

For gDNA sequencing of BLOC-1 subunits, we designed primers to cover all coding exons and flanking intronic regions of *BLOC1S1* (NT_029419.12), *BLOC1S2* (NT_030059.13), *BLOC1S3* (NT_011109.16), *CNO* (NT_006051.18), *DTNBP1* (NT_007592.15), *MUTED* (NT_007592.15), *PLDN* (NT_010194.17), and *SNAPIN* (NT_004487.19); primer sequences are shown in Table S1, available online. Direct sequencing was carried out with the di-deoxy termination method (ABI BigDye Terminator v3.1) on an ABI 3130xl DNA sequencer (Applied Biosystems, Austin, TX). Results were analyzed with Sequencher v4.9 software (Gene Codes Corporation, Ann Arbor, MI). The HPS-9 patient's mutation in *PLDN* was verified bidirectionally and based on the accession number NM_012388.2. For SNP genotyping, genomic DNA was run on a Human 1M-Duo DNA Analysis BeadChip, and the data were analyzed with the GenomeStudio software (both from Illumina, San Diego, CA).

RNA Analysis: Extraction, cDNA, and qRT-PCR

Total RNA was isolated from control and patient fibroblasts and melanocytes with the RNA-Easy Mini-Kit (QIAGEN) according to the manufacturer's protocol. RNA was treated with a DNase kit (DNA-free) according to the manufacturer's protocol (Applied Biosystems, Austin, TX) so that all remaining DNA could be removed. RNA concentrations and purity were measured on the Nanodrop ND-1000 apparatus (Nanodrop Technologies, Wilmington, DE). First-strand cDNA was synthesized with a high-capacity RNA-to-cDNA kit (Applied Biosystems) according to the manufacturer's guidelines. Human and fetal cDNA panels were purchased from Promega (Madison, WI). For tissue-specific cDNA expression studies (Figure 3B), primers specific to each *PLDN* transcript (transcript 1, *PLDN1,* NM_012388.2—forward primer across exon 3 and 4 boundary and reverse primer within exon 5; transcript 2, *PLDN2,* AK128626—forward primer in exon A and reverse primer across exon 2 and exon B boundary) and *GAPDH* (NM_002046.3) were designed and used for standard polymerase chain reaction (PCR) (primer sequences are shown in Table S2). For patient and control fibroblast and melanocyte cDNA analysis (Figure 3C), primers amplifying exclusively the entire coding region of either *PLDN1* or *PLDN2* were used. All PCR products were electrophoresed on 2% agarose gels. For quantitative real-time PCR (qRT-PCR), Taqman gene expression master mix reagent and Assays-On-Demand (Applied Biosystems) were obtained for *PLDN* (assay IDs Hs00202626_m1 and Hs01126975_m1) and a control gene, *GAPDH* (assay ID Hs99999905_m1). qRT-PCR was performed with 100 ng cDNA on an ABI PRISM 7900 HT Sequence Detection System (Applied Biosystems) by the comparative C_T method ($\Delta\Delta C_T$); this method measures relative gene expression.[14] The cycling conditions were as follows: 2 min at 50°C, 10 min at 95°C, and 40 cycles at 95°C for 15 s and 60°C for 60 s.

Plasmids

For cDNA constructs, forward and reverse primers were designed to include the native translation initiation (ATG) and termination codons, allowing ligation into the pCMV-Myc tag (C-terminal) expression vector (Clontech, Mountain View, CA) with EcoR1 and KpnI (5′ and 3′, respectively). Primer sequences are shown in Table S3. A full-length *PLDN* IMAGE cDNA clone (3450397) was purchased from Thermo Scientific (Waltham, MA), and the *PLDN*-Δ3 transcript was amplified from patient cDNA.

Antibodies

Mouse monoclonal antibodies against the following proteins were acquired as follows: syntaxin-13 (used for immunoblotting; clone 15G12, Abcam, Cambridge MA), Myc-tag (clone 9E10), β-actin (Clone AC-15), α-tubulin (clone B-5-1-2; all from Sigma Aldrich, St. Louis MO), TYRP1 (used for immunofluorescence and internalization assays; clone TA99, ATCC, Masasses VA), tyrosinase (clone T311, Santa Cruz Biotechnology, Santa Cruz, CA), and cappuccino (clone S-5; Santa Cruz Biotechnology). Rabbit polyclonal antibodies against the following proteins were acquired as follows: syntaxin-13 (used for immunofluorescence; Synaptic Systems GmbH, Goettingen Germany), PMEL-17 (Neomarkers, Fremont, CA), TYRP1 (used for immunoblotting) and HPS4 (both from Santa Cruz Biotechnology, Santa Cruz, CA), and HPS5 and snapin (both from ProteinTech, Chicago, IL). A sheep polyclonal antibody against TGN38 was obtained from AbD Serotec (Raleigh, NC), and a goat polyclonal antibody against EEA1 was purchased from Santa Cruz Biotechnology (Santa Cruz, CA). The mouse monoclonal antibody against pallidin was a kind gift from Dr. E. Dell'Angelica (UCLA School of Medicine, Los Angeles, CA).

Protein Extraction and Immunoblotting

Cells were grown to confluency in 25 cm^2 flasks, washed twice with ice-cold PBS, and scraped into 250 μl of cell lysis buffer containing 50 mM Tris-HCl (pH 7.5), 50 mM sodium fluoride, 5 mM sodium pyrophosphate, 1 mM sodium orthovanadate, 1 mM EDTA, 1 mM EGTA, 0.27 M sucrose, 1% Triton X-100, and Complete, Mini Protease Inhibitor Cocktail (Roche Diagnostics). Cell lysates were centrifuged (at 15,000 RPM for 15 min at 4°C); supernatants were removed for immunoblotting or coimmunoprecipitation experiments. Twenty micrograms of total protein, as determined by the Dc Protein assay (BioRad, Hercules, CA), were loaded onto 4%–20% Tris-Glycine gels. Proteins were blotted onto PVDF membranes (Invitrogen) for HRP detection or onto nitrocellulose membranes (Invitrogen) for Li-Cor detection. After blotting, membranes were probed with the appropriate antibodies, and loading was controlled by blotting of the same membranes with either α-tubulin or β-actin. HRP-conjugated secondary anti-mouse or anti-rabbit antibodies (Amersham Biosciences, Piscataway, NJ) and IRDye 800CW-conjugated secondary anti-mouse or anti-rabbit antibodies (Li-Cor Biosciences, Lincoln, NE) were used. The antigen-antibody complexes were visualized with an Enhanced Chemiluminescence (ECL) kit (Amersham Biosciences, Piscataway, NJ) or detected with the Li-Cor Odyssey Infrared imaging system. All blots were detected with HRP except for HPS5 and α-tubulin, where Li-Cor detection was used.

Coimmunoprecipitation and Plasma-Membrane Protein Biotinylation

For coimmunoprecipitation, 20 μg of anti-Myc monoclonal antibodies were covalently conjugated to 100 μl of Dynabeads Protein G (Invitrogen) with dimethyl pimelimidate and triethanolamine according to the manufacturer's instructions. Transfected control melanocytes growing in T25 flasks were harvested 48 hr after transfection, and proteins were extracted as described above. Extracted proteins (1 mg) were mixed with 20 μl of

antibody-conjugated Dynabeads and incubated on a blood rotor with end-over-end mixing (at 4°C for 3 hr). The complexes were then washed three times with cell lysis buffer supplemented with 150 mM NaCl, after which proteins were eluted by being boiled in 2× SDS loading buffer (10 min). The protein samples were loaded directly onto SDS-PAGE gels for immunoblotting analysis. For membrane protein biotinylation, control and patient melanocytes were incubated with 500 μl of 0.25 mg/ml EZ-Link Sulfo-NHS-SS-Biotin (Thermo Scientific, Waltham, MA) for 30 min at 4°C. This reaction was quenched by incubation with 1 M NH_4Cl for 5 min. Protein was then extracted via the protocol above. The biotin-labeled proteins were separated from the total lysates with streptavidin Dynabeads (Invitrogen, Carlsbad, CA) according to the manufacturer's instructions. The protein samples were loaded directly onto SDS-PAGE gels for immunoblotting analysis.

Immunofluorescence Microscopy

Cells were grown in four-well chamber slides, fixed with 4% paraformaldehyde, and permeabilized with 0.1% Triton X-100. Alexafluor 488 and 555 secondary antibody conjugates were purchased from Invitrogen (Carlsbad, CA), and nuclei were counterstained with DAPI (Vector Laboratories, Burlingame, CA). Cells were imaged with a Zeiss 510 META confocal laser-scanning microscope with the pinhole set to 1 Airy unit. A series of optical sections were collected from the *xy* plane and merged into maximum projection images.

TYRP1 Internalization Assay

This assay was carried out essentially as previously described.[15] In brief, control and HPS-9 patient melanocytes were trypsinized and washed twice with Ham's F10 medium containing 10% FBS and 25 mM HEPES. For each time point, 2×10^5 cells were used and incubated with a monoclonal antibody against TYRP1 on ice for 30 min so that antibody binding to plasma membrane TYRP1 could take place. Cells were then washed twice with medium and transferred to 37°C for different amounts of time (0, 5, 10, 15, 30, and 60 min), after which they were incubated on ice with Alexafluor-488-conjugated secondary antibodies for 30 min. The cells were then washed twice with medium and resuspended in FACS buffer (5% FBS, 1 mM EDTA in 1× PBS). The samples were sorted on a Becton Dickenson FACSCalibur flow cytometer, and the amount of green fluorescence was counted and analyzed with FlowJo software.

Results

BLOC-1 Mutation Screen

We screened 38 patients with HPS-like symptoms but no mutations associated with *HPS1–6*. We completely sequenced the exonic regions of all eight BLOC-1 subunit-encoding genes and found a single HPS–8 patient with a mutation in *BLOS3*; this patient will be described elsewhere. However, we also identified another unique patient with a nonsense mutation (c.232C>T; p.Gln78Och) in exon 3 of the pallidin-encoding gene, *PLDN* (Figure 1A), and we can thus define a new HPS subtype, HPS-9. The patient's mutation was homozygous, despite no known relationship between the parents. A SNP-chip microarray identified homozygosity within the region of the *PLDN* locus on chromosome 15q21.1 (Figure 1B), suggesting distant consanguinity; there was only one other region of extended homozygosity, on chromosome 6p22.1 (Figure 1C).

Clinical Features

The patient, a 9-month-old male of Indian ancestry, presented at birth with generalized hypopigmentation and respiratory distress requiring a 3 week admission to a neonatal intensive-care unit for respiratory support. Molecular testing for oculocutaneous albinism (OCA) types 1 and 3 was negative (OCA-1 and OCA-3; MIM 606933 and 203290). Nystagmus, iris transillumination, and retinal hypopigmentation were noted upon examination at 3 months (Figure 2A). Upon evaluation at the NIH Clinical Center at 9 months, platelet electron microscopy showed absent platelet delta granules, consistent with HPS (Figure 2B). Growth, development, and general health were normal, and there was no history of severe or unusual infections, easy bruising, or bleeding. The irides were pale blue. Nystagmus was present. No excessive ecchymoses were observed. Polymorphonuclear leukocyte granules were morphologically normal. The hair was blond and silvery (Figure 2A); hair microscopy showed reduced pigment relative to ethnic background, but no unusual pigment clumping (Figure 2C). Cultured melanocytes reflected the reduction in pigment (Figure 2D).

PLDN Transcripts

PLDN has two known human mRNA transcripts. Transcript 1 contains five coding exons (AF080470), and transcript 2 has three coding exons (AK128626); only exon 2 is shared by both transcripts (Figure 3A). Investigation of the expression pattern of both transcripts across a variety of adult and fetal tissues (Figure 3B) showed ubiquitous expression of transcript 1, with the notable exception of both adult and fetal brain, consistent with previous reports.[16,17] In contrast, transcript 2 was expressed only in adult brain, testis, and leukocytes and in fetal brain, lung, and thymus.

Our patient's mutation involves *PLDN* exon 3, which is present only in transcript 1, so transcript 2 should not be affected. Transcript 2 is not expressed in normal fibroblasts or melanocytes (Figure 3C), and we also demonstrate that its expression is not upregulated as a compensatory mechanism in the patient's cells (Figure 3C), suggesting that transcripts 1 and 2 have different promoters and different functions within cells. Quantitative real-time PCR analysis of transcript 1 revealed normal *PLDN* mRNA expression in the patient's fibroblasts (97.2% ± 3.8%) and melanocytes (97.9% ± 4.2%) compared to controls. This finding was confirmed by the fact that standard PCR with cDNA exclusive primers for transcript 1 gave bands of equal intensity (Figure 3C). This suggests that nonsense-mediated mRNA decay is not occurring for this mutation, probably because

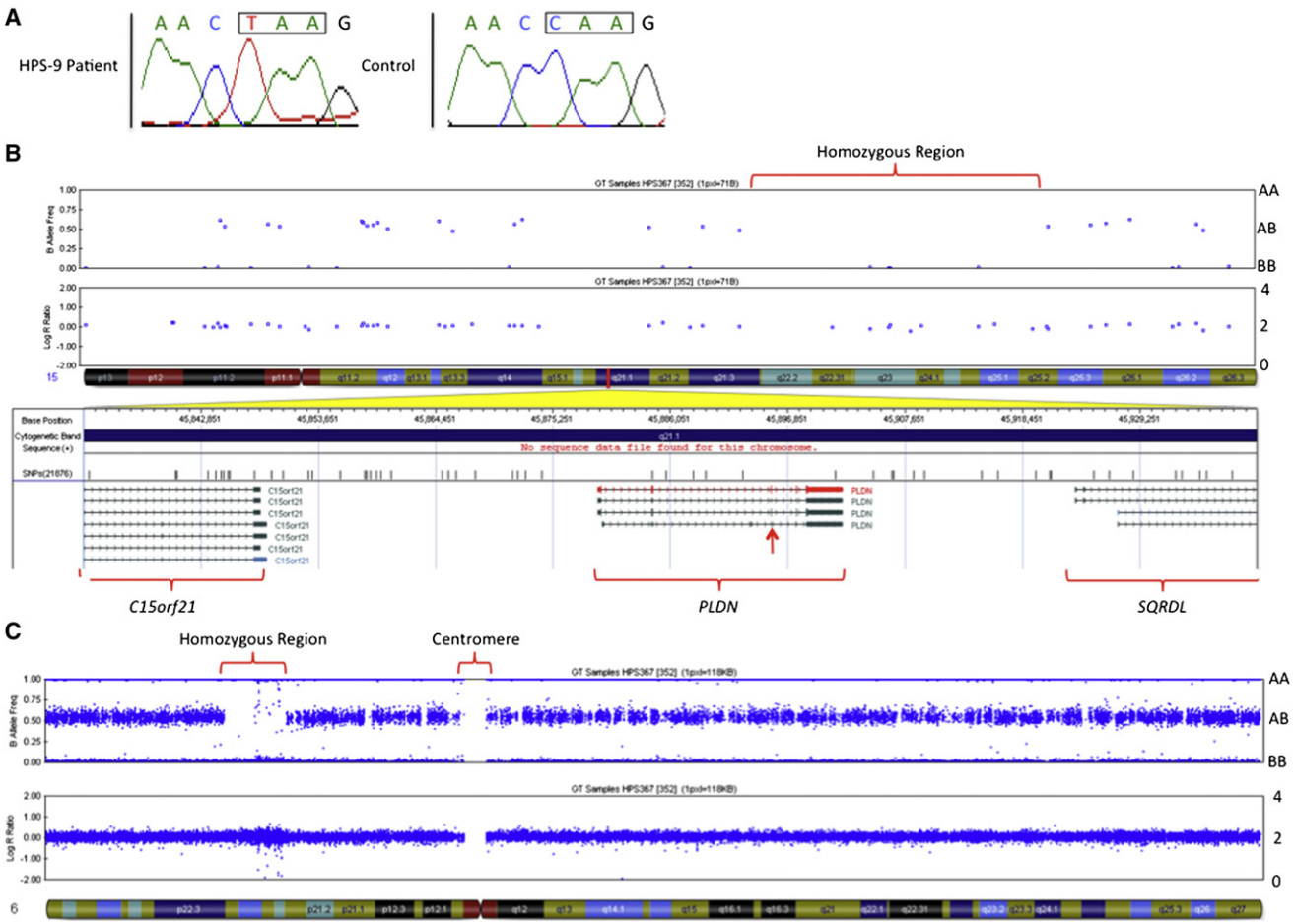

Figure 1. Molecular Aspects of the HPS-9 Patient
(A) Sequencing chromatograms from control and patient genomic DNA. The patient is homozygous for c.232C>T in exon 3 of *PLDN*.
(B) SNP-array data for the HPS-9 patient. An enlarged region of the *PLDN* locus on chromosome 15 shows homozygosity (red bracket) and the position of the mutation (arrow).
(C) SNP-array data for the HPS-9 patient showing a chromosome 6p22 region that is the only region of extended homozygosity (red bracket) in his genome. On the B allele plots (upper charts), the middle represents heterozygosity (AB), and the edges represent homozygosity (AA or BB). The log R ratio plots (lower charts) show that there are normal SNP calls in both of these regions, indicating that no deletions or insertions are present.

the mutation is close to (8 bp away from) an intron-exon boundary.[18]

Surprisingly, cDNA amplification results showed an additional weak band in the patient (Figure 3C), suggesting an alternative splicing event. Although the NetGene2 splice-site prediction tool did not predict additional splice sites due to the mutation, the Exonic Splicing Enhancers (ESE) finder tool indicated that c.232C>T would abolish a SC35 binding site in the DNA; abolishment of this binding site is predicted to result in the skipping of exon 3.[19] Indeed, sequencing of the patient's additional smaller PCR band revealed the absence of exon 3, including the nonsense mutation (Figure 3D). Removal of exon 3 (88 bp) puts exon 4 out of frame, which might introduce susceptibility to nonsense-mediated decay or create an alternate protein consisting of 86 amino acids: 74 of the original pallidin N-terminal amino acids encoded by exons 1 and 2 and then 12 alternate amino acids encoded by exon 4.

Instability of the BLOC-1 Complex

Despite normal *PLDN* mRNA expression of transcript 1, immunoblot analysis showed that pallidin was present in control fibroblasts but was absent from HPS-9 fibroblasts, indicating an unstable mutant pallidin protein in the patient's cells (Figure 4A). Conversely, pallidin was present in fibroblasts of HPS patients containing BLOC-2 or BLOC-3 mutations, suggesting that these complexes assemble independently of BLOC-1.

Despite the existence of an interactome map of BLOC-1's constituent proteins,[20] little is known about the function of the complex. To address this, we determined the presence of other members of the BLOC-1 complex with available antibodies. In the HPS-9 fibroblasts, cappuccino was absent and snapin was significantly reduced (Figure 4B), indicating that pallidin is required to stabilize the BLOC-1 complex.

Pallidin comprises of 172 amino acids and shares no homology to any known protein. The first 60 amino

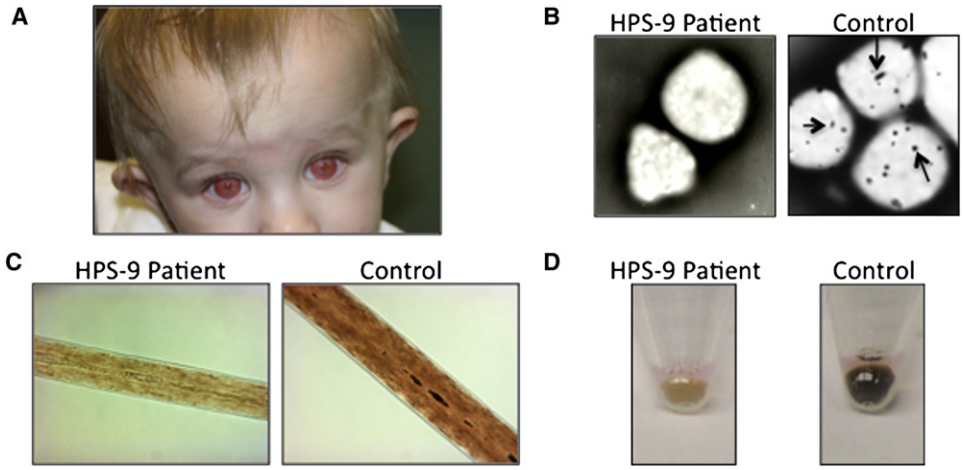

Figure 2. Clinical Aspects of the HPS-9 Patient
(A) The patient has iris transillumination and fair skin and hair.
(B) Whole-mount electron microscopy of the patient's platelets revealed no delta granules, which are present in control platelets (arrows).
(C) Hair shafts show reduced pigmentation in the patient compared to the control, but no abnormal clumping of pigment was seen.
(D) Packed melanocytes show negligible pigment in the HPS-9 patient compared to an ethnically matched control (right panels).

acids give rise to an unstructured protein, followed by two highly α-helical coiled-coil regions (amino acids 60–100 and 109–172; Figure 4C). The two coiled-coil regions have been shown to be essential for pallidin to bind to itself and to syntaxin-13, an early endosomal t-SNARE.[16] Furthermore, syntaxin-13 expression is reduced in cells of the *pallid* mouse,[16,17] Similarly, our patient's melanocytes revealed a weaker-than-normal signal for syntaxin-13 but normal localization by immunofluorescence microscopy (Figure 4D). Immunoblots and densitometry showed a 46% reduction in syntaxin-13 levels in the HPS-9 cells compared to controls (Figure 4E), indicating that pallidin might be required for syntaxin-13's stability, and possibly its correct function, at least for the syntaxin 13's cellular portion that associates with BLOC-1.

To discern the effect of the alternative transcript that our patient's mutation creates, we cloned the full-length *PLDN* (PLDN-FL) and the alternative transcript with the splice variant (deleting exon 3; PLDN-Δ3) into the pCMV-Myc tag vector. When overexpressed in melanocytes, both the PLDN-FL and PLDN-Δ3 constructs localized to EEA1-positive early endosomes (Figure 4F), as predicted for BLOC-1 components.[15] Expression of the Myc-PLDN constructs in the HPS-9 patient melanocytes showed that the PLDN-FL, but not the PLDN-Δ3 constructs, increased the levels of both cappuccino and snapin to near normal levels in HPS-9 melanocytes (Figure 4G). Furthermore, PLDN-FL expression rescued the amount of pigment in the packed melanocyte pellets (Figure 4H). Coimmunoprecipitation studies with Myc-tag antibodies in normal melanocytes showed that PLDN-FL, but not the PLDN-Δ3 construct, interacted with endogenous syntaxin-13 (Figure 4I).

Defects in Melanin Biogenesis

Another measure of function involves the ability of melanogenic proteins such as tyrosinase, TYRP1 (mutated in OCA-1 and OCA-3, respectively), and PMEL-17 to traffic to melanosomes for melanin synthesis.[1,10] We observed a normal, dispersed cytoplasmic distribution of the stage I and II melanosome marker PMEL17 in the HPS-9 patient's melanocytes (Figure 5A), suggesting correct biogenesis of these early melanosomal organelles. Early melanosomes mature into stage III melanosomes by acquiring other melanogenic proteins, such as TYRP1 and tyrosinase, which are crucial for melanin production, and the eventual result is melanin-laden stage IV melanosomes required for pigmentation. This maturation is coupled with the gradual reduction of PMEL-17 on the melanosomes. We found that TYRP1 abnormally accumulated in the Golgi region and occasionally localized to non-Golgi-associated punctate perinuclear structures and the plasma membrane in HPS-9 cells (Figure 5B). In contrast, tyrosinase appeared to partially localize to PMEL-17-labeled structures in the HPS-9 melanocytes, as in control cells (data not shown), and did not appear to significantly accumulate in the Golgi region (Figure 5C), suggesting that the mislocalization in pallidin-deficient cells is cargo specific. On closer investigation of the non-Golgi punctate structures of TYRP1, we found that some of the TYRP1 colocalized with the syntaxin-13-positive early endosomes in patient cells only (Figure 5D), suggesting the mis-sorting of TYRP1 into the early endosomal compartment.

Previous studies of BLOC-1-deficient mouse melanocytes showed enhanced flux of TYRP1 through the plasma membrane and decreased steady-state TYRP1 levels as a result of lysosomal degradation of mis-trafficked TYRP1.[15] Our studies of HPS-9 melanocytes yielded similar

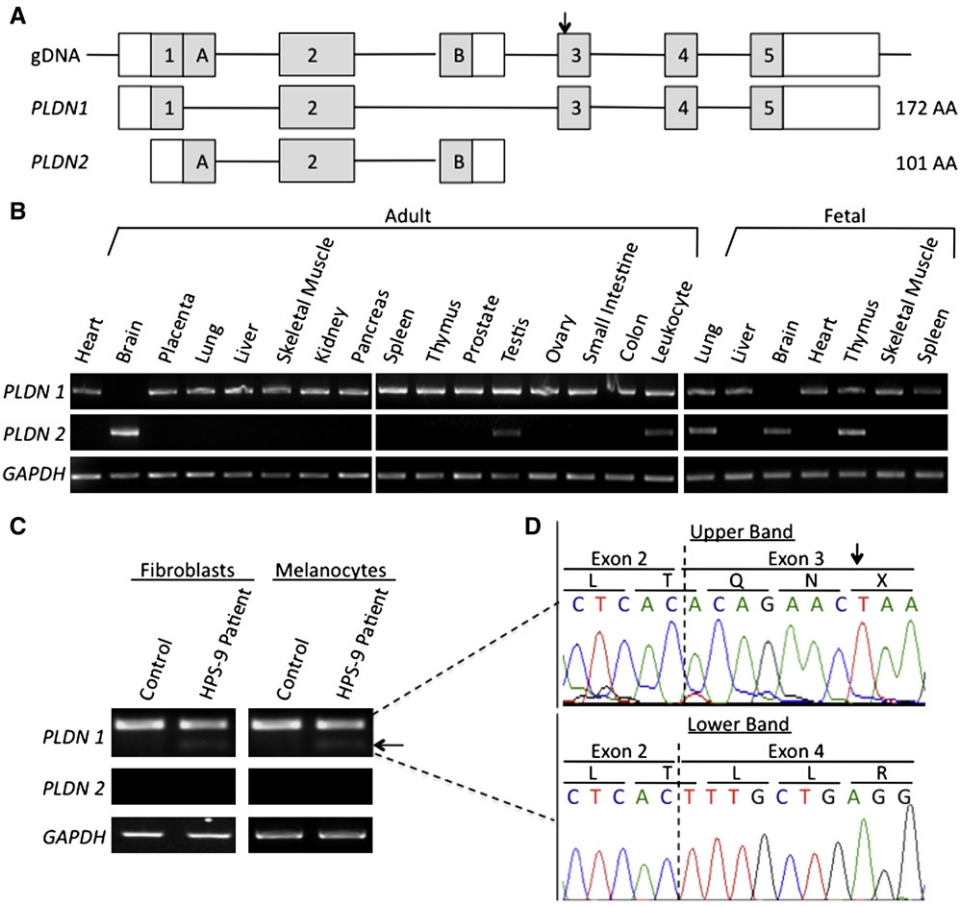

Figure 3. *PLDN* mRNA Transcripts
(A) Exon structure of *PLDN* at the gDNA and mRNA transcript levels. *PLDN* transcript 1 (*PLDN1*, encoding 172 amino acids (AA)) and transcript 2 (*PLDN2*, encoding 101 AA) have only exon 2 in common. White boxes, untranslated exonic regions; gray boxes, coding exonic regions; black arrow, position of the HPS-9 patient's mutation. "A" and "B" represent exons that were identified after the initial assignment of exon numbers.
(B) PCR amplification shows ubiquitous expression of *PLDN1* but a notable absence in both adult and fetal brain. *PLDN2* has a more limited expression pattern. Amplification of *GAPDH* shows equal loading.
(C) Agarose gel images of fibroblast and melanocyte cDNA *PLDN* transcript amplifications. A faint lower band of *PLDN1* is detected in the patient only (arrow). No upregulation of *PLDN2* is seen. Loading was controlled by *GAPDH*.
(D) Sequencing chromatograms of the *PLDN1* upper and lower bands from (C) show homozygous presence of the mutation in exon 3 in the upper band (upper panel, arrow) and complete splicing out of exon 3 in the lower, faint band (lower panel). A dotted line represents the exon-exon boundary.

results: Steady-state TYRP1 levels were decreased in the patient's melanocytes by immunofluorescence microscopy and immunoblotting (Figures 5B and 5E). By biotinylating the surface proteins before cell lysis, we showed that TYRP1 was significantly increased in the patient's plasma membrane protein fraction (Figure 5E), and the patient's melanocytes had a reduced rate of TYRP1 endocytosis in comparison to that of control cells (Figure 5F).

Discussion

Here we report a case of HPS-9 in an infant with albinism and without platelet delta granules. Our patient had no clinical signs of additional HPS subtype-specific symptoms, such as immunodeficiency, granulomatous colitis, or pulmonary fibrosis. Some of these symptoms can develop at a later age; therefore, following the clinical course of this patient as he grows older will be crucial.

Basic studies indicated that our patient exhibited a homozygous nonsense mutation in *PLDN*, whose protein product, pallidin, is a member of the BLOC-1 complex. This mutation affects only transcript 1 of *PLDN*, which has a ubiquitous pattern of expression in adult and fetal tissues, with the notable exception of both adult and fetal brain. The strong expression of *PLDN* transcript 2, coupled with the absence of transcript 1 in the brain, might reflect the existence of a neuronal pallidin isoform and suggests that different promoters for these transcripts might allow differential tissue expression, such as in the brain. Furthermore, *PLDN* transcript 2 is not expressed in fibroblasts or melanocytes and does not become upregulated as a result of the mutation present in transcript 1 in our patient; consequently, we speculate that this isoform has a different

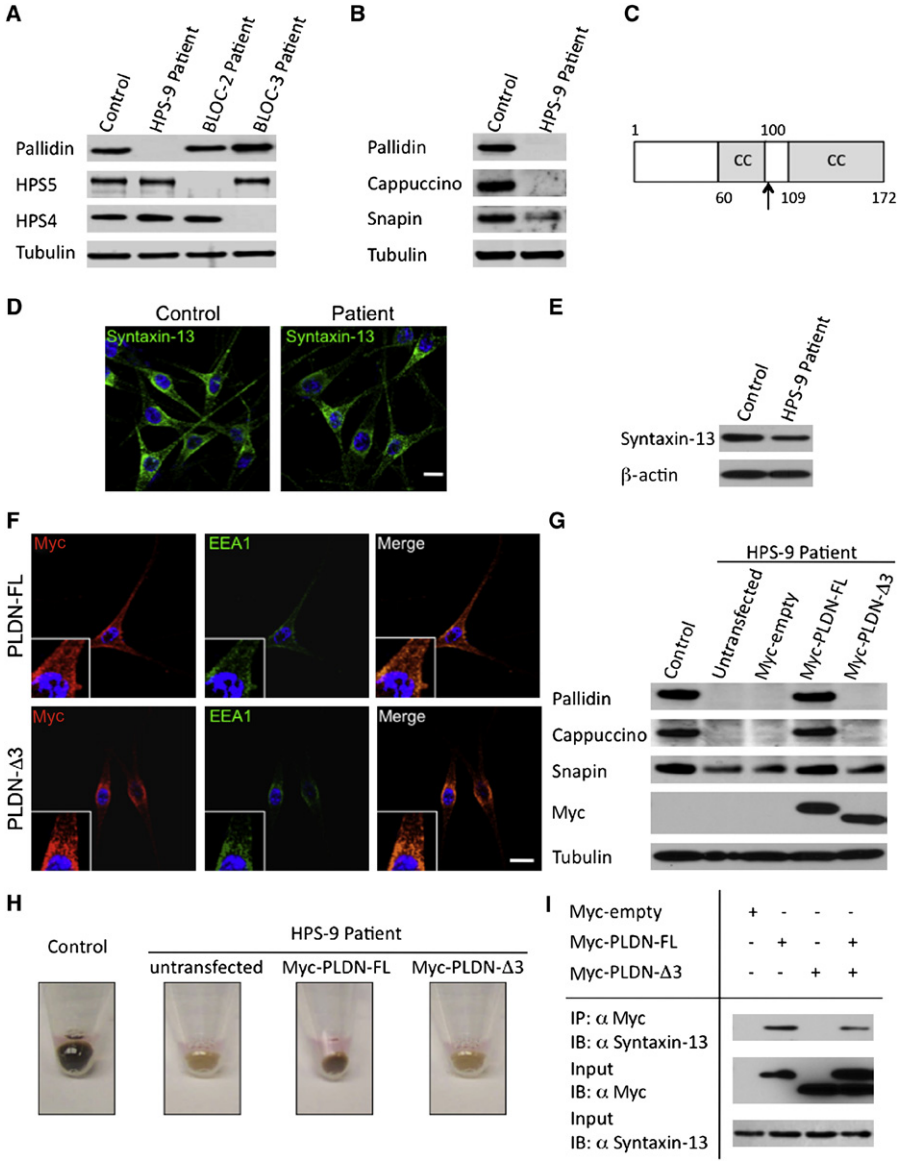

Figure 4. Cellular Studies of HPS-9 Fibroblasts and Melanocytes

(A) Immunoblots of fibroblast extracts of the HPS-9 patient and BLOC-2 and BLOC-3 patients treated with pallidin (BLOC-1), HPS5 (BLOC-2), and HPS4 (BLOC-3) antibodies. Only the HPS-9 patient showed absence of the pallidin protein. The loading control was β-tubulin.

(B) Immunoblots of control and HPS-9 patient fibroblast lysates treated with antibodies to the BLOC-1 subunits pallidin, cappuccino, and snapin. Pallidin and cappuccino were undetectable, and snapin was significantly reduced in the HPS-9 patient compared to the control. Loading was controlled by β-tubulin.

(C) Schematic depiction of the pallidin protein structure. Amino acids 1–60 and 100–109 are unstructured. Highly α-helical and coiled-coil (CC; gray boxes) regions are within amino acids 60–100 and 109–172. The HPS-9 patient's p.Gln78Och mutation is indicated (arrow).

(D) Immunofluorescence images of syntaxin-13 in both control and HPS-9 melanocytes. Syntaxin-13 signal appeared weaker in the patient than in the control but has the same cellular localization pattern.

(E) An immunoblot with syntaxin-13 antibodies showed reduced expression in the HPS-9 patient compared to the control. Loading was controlled by β-actin.

(F) Microscopic images of control melanocytes transfected with Myc-tagged full-length (PLDN-FL) and the truncated (PLDN-Δ3) versions of *PLDN* showed localization of both to EEA1-positive early endosomes.

(G) Immunoblots of lysates from control and transfected HPS-9 patient melanocytes treated with antibodies to the BLOC-1 subunits pallidin, cappuccino, and snapin. Pallidin, cappuccino, and snapin were returned to near normal levels in only the HPS-9 cells transfected with the PLDN-FL construct. Loading was controlled by β-tubulin, and expression of the Myc-tag constructs is shown.

(H) Packed melanocytes show negligible pigment in the HPS-9 patient without transfection (see also Figure 3D); only the Myc-PLDN-FL construct could rescue the production of pigment in the patient's melanocytes. (I) Coimmunoprecipitation showed that PLDN-FL could pull down syntaxin-13, but neither the empty plasmid nor the PLDN-Δ3 version could, despite confirmation that they were expressed and synaxin-13 was present in the lysate. A combination of PLDN-FL and PLDN-Δ3 could also pull down syntaxin-13. For all microscopic images, nuclei were stained with DAPI (blue); scale bars represent 20 μm.

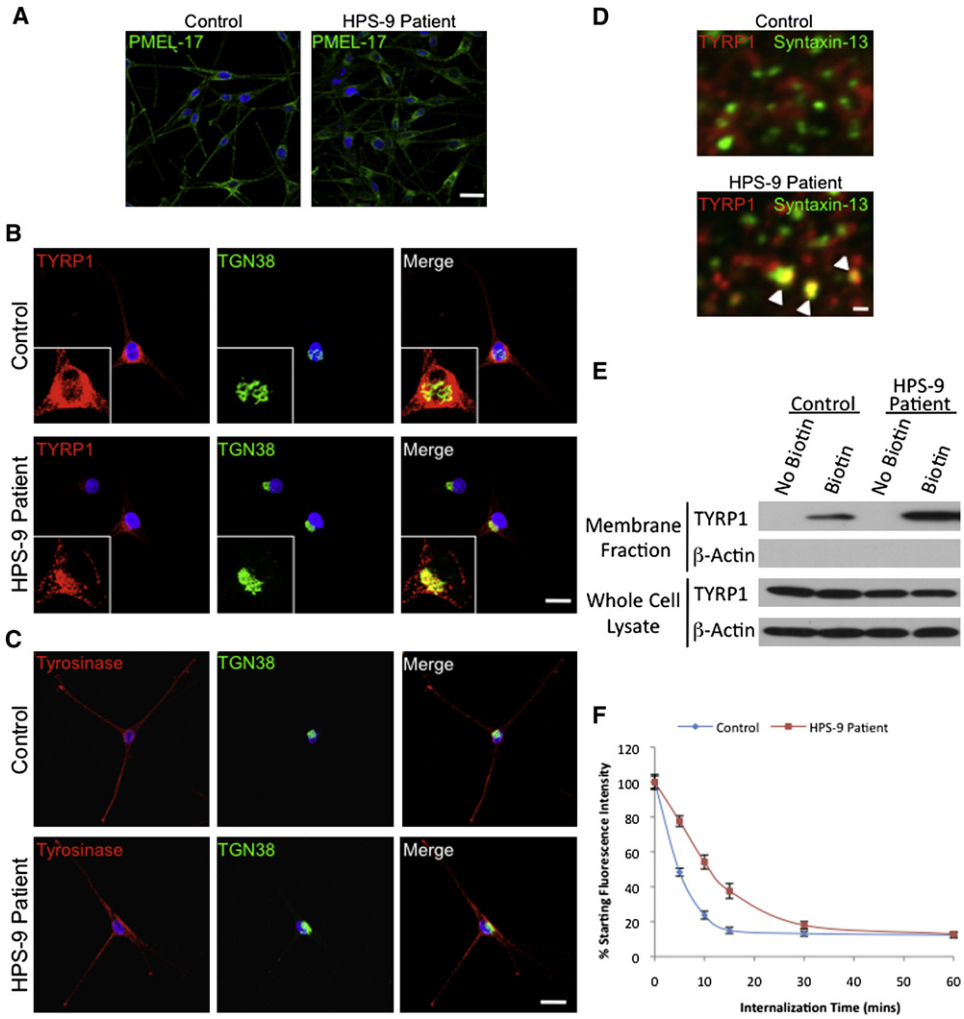

Figure 5. Pigment-Biosynthesis Defects in HPS-9

(A) Immunofluorescence images of PMEL-17 in both control and patient melanocytes. A normal dispersed cytoplasmic distribution is visible in the patient's cell. PMEL17 is a marker for stage I and II melanosomes, indicating correct biogenesis of these early melanosomal organelles in the patient's cells.

(B) Immunofluorescence images of TYRP1 and the Golgi marker TGN38 in control and the HPS-9 patient's melanocytes. TYRP1 is localized to punctate structures throughout the cytoplasm of control cells. The patient's cells showed reduced TYRP1 expression and aberrant TYRP1 localization mainly in the Golgi region (inserts).

(C) Immunofluorescence images of tyrosinase and TGN38. Tyrosinase distribution appeared normal in HPS-9 melanocytes. For the above microscopy images, nuclei were stained with DAPI (blue); scale bars represent 20 μm.

(D) Enlarged immunofluorescence images of control and HPS-9 melanocytes stained for TYRP1 and syntaxin-13 show occasional colocalization in patient cells only. Scale bars represent 5 μm.

(E) Plasma-membrane protein-biotinylation assay. The HPS-9 patient's cells showed a significant increase of TYRP1 on the plasma membrane in comparison to the control. No β-actin was detected in the membrane fraction (demonstrating purity). Whole-cell lysates showed equal TYRP1 expression in control cells and the HPS-9 patient's cells (loading was controlled by β-actin).

(F) An TYRP1 internalization assay as a function of time shows a decreased rate of endocytosis from the plasma membrane in the patient's melanocytes compared to control cells. Values shown are mean percentages of the initial amount of TYRP1 on the membrane, and error bars represent ± 1 standard error of the mean ($n = 3$).

function within cells and that this function is potentially distinct from a role in the BLOC-1 complex. It has previously been reported that snapin performs an autophagy function in the brain,[21] and alterations in dysbindin have been associated with schizophrenia,[22] suggesting that other BLOC-1 subunits might exhibit dual functions.

Although eight genes encode the BLOC-1 complex and there are five HPS mouse models with mutations in BLOC-1 genes,[11] only three BLOC-1 human mutations, including those in the patient presented here, have been identified.[7,8] Taken together, the data presented here suggest that the proteins that constitute the BLOC-1 complex perform varied and essential functions in many tissue types, potentially as a result of alternative transcripts. Therefore, mutations in these genes are more than likely to affect only transcripts that are not essential for development and survival in humans, explaining why only a few mutations have been identified to date. In the case of

pallidin, we might never find a human with a mutation that would affect transcript 2 because such a mutation might be lethal. On the other hand, the failure to identify other BLOC-1 defects in humans might reflect our ignorance of the additional functions of BLOC-1 subunits or simply a redundancy of the proteins performing these functions.

The absence of pallidin in the patient's melanocytes destabilized other BLOC-1 subunits; decreased syntaxin-13-BLOC-1 binding; caused mistrafficking of TYRP1, which accumulated in the Golgi region, the early endosome compartment, and cell membrane; and severely reduced pigment production. The decreased rate of endocytosis of TYRP1 from the plasma membrane could be due to the increased amount of TYRP1 present on the membrane, resulting in saturation of the endocytic recycling machinery. It is unknown whether the primary trafficking defect associated with BLOC-1 deficiency is mis-localization of TYRP1 to the plasma membrane or to the early endosomal compartment. Increased accumulation of plasma membrane TYRP1, and the resulting saturated endocytic recycling machinery, could explain the presence of TYRP1 in the syntaxin-13-positive early endosomes, suggesting that TYRP1 trafficking to the plasma membrane is the primary defect. However, it is also possible that mis-sorting of TYRP1 into syntaxin-13-positive early endosomes leads to increased TYRP1 on the cell surface as a secondary defect.[23] We and others[15,23] favor the second hypothesis because disrupting the biosynthetic pathway by Golgi disruption in BLOC-1-deficient mouse melanocytes did not significantly reduce the amount of TYRP1 on the membrane; this suggests the TYRP1 is derived primarily from the recycling and endosomal compartments.[15] Furthermore, the facts that the BLOC-1 complex, specifically pallidin, interacts with syntaxin-13 and that cargo are mis-sorted into these syntaxin-13-positive vesicles suggests that the BLOC-1 complex might function to prevent the delivery of certain proteins to the early endosomal compartment. This would allow these proteins to be properly diverted to melanosomes and other lysosome-related organelles, as required.

In many respects, the phenotype of our HPS-9 patient's cells resembles that of BLOC-1-deficient mouse melanocytes, in which immuno-electron microscopy showed normal PMEL17 and tyrosinase distribution but TYRP1 accumulation within tubulovesicular structures and early vacuolar endosomes near the Golgi.[15] We conclude that aberrant TYRP1 trafficking probably contributes to the hypopigmentation of our patient. However, a more complete appreciation of the ramifications of pallidin deficiency awaits the identification and evaluation of additional HPS-9 patients.

Supplemental Data

The supplemental data include three tables giving the sequences of all primers used for this article and can be found with this article online at http://www.cell.com/AJHG/.

Acknowledgments

We appreciate the excellent technical assistance of Roxanne Fischer. We thank Thomas Markello and Hannah Carlson-Donohoe for assistance with SNP arrays and E. Dell'Angelica for supplying the pallidin antibody. This study was supported by the Intramural Research Programs of the National Human Genome Research Institute, National Institutes of Health, Bethesda, MD, USA. All authors declare no conflicts of interest.

Received: March 11, 2011
Revised: May 4, 2011
Accepted: May 9, 2011
Published online: June 9, 2011

Web Resources

The URLs for data presented herein are as follows:

Ensembl, http://ensembl.org
Exonic Splicing Enhancers (ESE), http://genes.mit.edu/burgelab/rescue-ese
NetGene2, http://www.cbs.dtu.dk/services/NetGene2
NIH Clinical Trials, www.clinicaltrials.gov
Online Mendelian Inheritance in Man (OMIM), http://www.omim.org
Primer3, http://frodo.wi.mit.edu/primer3

References

1. Huizing, M., Helip-Wooley, A., Westbroek, W., Gunay-Aygun, M., and Gahl, W.A. (2008). Disorders of lysosome-related organelle biogenesis: Clinical and molecular genetics. Annu. Rev. Genomics Hum. Genet. *9*, 359–386.
2. Oh, J., Bailin, T., Fukai, K., Feng, G.H., Ho, L., Mao, J.I., Frenk, E., Tamura, N., and Spritz, R.A. (1996). Positional cloning of a gene for Hermansky-Pudlak syndrome, a disorder of cytoplasmic organelles. Nat. Genet. *14*, 300–306.
3. Dell'Angelica, E.C., Shotelersuk, V., Aguilar, R.C., Gahl, W.A., and Bonifacino, J.S. (1999). Altered trafficking of lysosomal proteins in Hermansky-Pudlak syndrome due to mutations in the beta 3A subunit of the AP-3 adaptor. Mol. Cell *3*, 11–21.
4. Anikster, Y., Huizing, M., White, J., Shevchenko, Y.O., Fitzpatrick, D.L., Touchman, J.W., Compton, J.G., Bale, S.J., Swank, R.T., Gahl, W.A., and Toro, J.R. (2001). Mutation of a new gene causes a unique form of Hermansky-Pudlak syndrome in a genetic isolate of central Puerto Rico. Nat. Genet. *28*, 376–380.
5. Suzuki, T., Li, W., Zhang, Q., Karim, A., Novak, E.K., Sviderskaya, E.V., Hill, S.P., Bennett, D.C., Levin, A.V., Nieuwenhuis, H.K., et al. (2002). Hermansky-Pudlak syndrome is caused by mutations in HPS4, the human homolog of the mouse light-ear gene. Nat. Genet. *30*, 321–324.
6. Zhang, Q., Zhao, B., Li, W., Oiso, N., Novak, E.K., Rusiniak, M.E., Gautam, R., Chintala, S., O'Brien, E.P., Zhang, Y., et al. (2003). Ru2 and Ru encode mouse orthologs of the genes mutated in human Hermansky-Pudlak syndrome types 5 and 6. Nat. Genet. *33*, 145–153.
7. Li, W., Zhang, Q., Oiso, N., Novak, E.K., Gautam, R., O'Brien, E.P., Tinsley, C.L., Blake, D.J., Spritz, R.A., Copeland, N.G., et al. (2003). Hermansky-Pudlak syndrome type 7 (HPS-7) results from mutant dysbindin, a member of the biogenesis of lysosome-related organelles complex 1 (BLOC-1). Nat. Genet. *35*, 84–89.

8. Morgan, N.V., Pasha, S., Johnson, C.A., Ainsworth, J.R., Eady, R.A., Dawood, B., McKeown, C., Trembath, R.C., Wilde, J., Watson, S.P., and Maher, E.R. (2006). A germline mutation in BLOC1S3/reduced pigmentation causes a novel variant of Hermansky-Pudlak syndrome (HPS8). Am. J. Hum. Genet. *78*, 160–166.
9. Wei, M.L. (2006). Hermansky-Pudlak syndrome: a disease of protein trafficking and organelle function. Pigment Cell Res. *19*, 19–42.
10. Raposo, G., Tenza, D., Murphy, D.M., Berson, J.F., and Marks, M.S. (2001). Distinct protein sorting and localization to premelanosomes, melanosomes, and lysosomes in pigmented melanocytic cells. J. Cell Biol. *152*, 809–824.
11. Li, W., Rusiniak, M.E., Chintala, S., Gautam, R., Novak, E.K., and Swank, R.T. (2004). Murine Hermansky-Pudlak syndrome genes: regulators of lysosome-related organelles. Bioessays *26*, 616–628.
12. Ilardi, J.M., Mochida, S., and Sheng, Z.H. (1999). Snapin: A SNARE-associated protein implicated in synaptic transmission. Nat. Neurosci. *2*, 119–124.
13. Huang, L., Kuo, Y.M., and Gitschier, J. (1999). The pallid gene encodes a novel, syntaxin 13-interacting protein involved in platelet storage pool deficiency. Nat. Genet. *23*, 329–332.
14. Livak, K.J., and Schmittgen, T.D. (2001). Analysis of relative gene expression data using real-time quantitative PCR and the 2(-Delta Delta C(T)) method. Methods *25*, 402–408.
15. Setty, S.R., Tenza, D., Truschel, S.T., Chou, E., Sviderskaya, E.V., Theos, A.C., Lamoreux, M.L., Di Pietro, S.M., Starcevic, M., Bennett, D.C., et al. (2007). BLOC-1 is required for cargo-specific sorting from vacuolar early endosomes toward lysosome-related organelles. Mol. Biol. Cell *18*, 768–780.
16. Moriyama, K., and Bonifacino, J.S. (2002). Pallidin is a component of a multi-protein complex involved in the biogenesis of lysosome-related organelles. Traffic *3*, 666–677.
17. Falcón-Pérez, J.M., Starcevic, M., Gautam, R., and Dell'Angelica, E.C. (2002). BLOC-1, a novel complex containing the pallidin and muted proteins involved in the biogenesis of melanosomes and platelet-dense granules. J. Biol. Chem. *277*, 28191–28199.
18. Maquat, L.E. (2004). Nonsense-mediated mRNA decay: Splicing, translation and mRNP dynamics. Nat. Rev. Mol. Cell Biol. *5*, 89–99.
19. Cartegni, L., Chew, S.L., and Krainer, A.R. (2002). Listening to silence and understanding nonsense: exonic mutations that affect splicing. Nat. Rev. Genet. *3*, 285–298.
20. Li, W., Feng, Y., Hao, C., Guo, X., Cui, Y., He, M., and He, X. (2007). The BLOC interactomes form a network in endosomal transport. J. Genet. Genomics *34*, 669–682.
21. Yuzaki, M. (2010). Snapin snaps into the dynein complex for late endosome-lysosome trafficking and autophagy. Neuron *68*, 4–6.
22. Ghiani, C.A., Starcevic, M., Rodriguez-Fernandez, I.A., Nazarian, R., Cheli, V.T., Chan, L.N., Malvar, J.S., de Vellis, J., Sabatti, C., and Dell'Angelica, E.C. (2010). The dysbindin-containing complex (BLOC-1) in brain: developmental regulation, interaction with SNARE proteins and role in neurite outgrowth. Mol. Psychiatry *15*, 115, 204–215.
23. Di Pietro, S.M., Falcón-Pérez, J.M., Tenza, D., Setty, S.R., Marks, M.S., Raposo, G., and Dell'Angelica, E.C. (2006). BLOC-1 interacts with BLOC-2 and the AP-3 complex to facilitate protein trafficking on endosomes. Mol. Biol. Cell *17*, 4027–4038.